Sang-Soon Kim, Won Choi, Sang-Hyun Park and Dong-Hyun Kang*

Mathematical modeling of ohmic heating for inactivation of acid-adapted foodborne pathogens in tomato juice

https://doi.org/10.1515/ijfe-2019-0388
Received December 30, 2019; accepted March 12, 2020; published online April 13, 2020

Abstract: The objective of the present study was to predict the inactivation trends of acid-adapted foodborne pathogens in tomato juice by ohmic heating through a numerical analysis method. The mathematical model based on finite element method (FEM) was used to simulate the multi-physics phenomena including electric heating, heat transfer, fluid dynamics, and pathogen inactivation. A cold spot was observed in the corner part of the ohmic heating chamber, where some pathogens survived even though all pathogens were inactivated elsewhere. Challenges of this study were how to reflect the increased resistance of pathogen by acid-adaptation. After simulation, we verified that inactivation level of acid-adapted foodborne pathogens by 25 V_{rms}/cm ohmic heating (1 kHz), predicted with the developed mathematical model, had no significant differences with experimental results ($p > 0.05$). Therefore, the mathematical approaches described in the present study will help juice processors determine the processing conditions necessary to ensure microbial safety at the cold point of a rectangular type batch ohmic heater.

Keywords: acid-adaptation; foodborne pathogen; mathematical modeling; ohmic heating; tomato juice.

1 Introduction

As minimal processing has been spotlighted in recent years to preserve food quality, food processing technology continuously advances to ensure safety with the least treatment. In this regard, novel thermal and non-thermal technologies have been introduced, which minimize quality degradation. Ohmic heating is thermal technology ensuring relatively uniform and rapid heating by means of electric current through food samples with lower capital cost compared to industrial microwave and radio frequency heating [1]. Even though several factors affect the performance of ohmic heating, it has been reported that food quality can be improved by ohmic rather than conventional heating [2, 3]. Foodborne pathogens would be inactivated rapidly with ohmic heating by means of the rapid and uniform heating, and also non-thermal bactericidal effect would accelerate the pathogen inactivation efficacy [4].

Predicting microbial destruction in thermal processing of foods has been a topic of intense investigation. The resistance of each pathogen to different lethal temperatures should be identified to predict the microbial destruction by thermal processing. Because most microorganisms are known to be destructed exponentially at lethal temperature, D-value, the time required to reduce the population of a microbe by 90% at isothermal heating conditions, is widely used as an indicator of thermal resistance of pathogens. D-values are usually calculated empirically because the values differ significantly according to the type of pathogen, nutritional components, pH, and viscosity of food samples [5, 6]. After D-values at various temperatures are determined, z-value, another heat resistance indicator, is calculated from the D-values. Subsequently, lethality (F value) is determined from the heating rate, thermal history, and the z-value to predict microbial destruction in thermal processing. These D- and z-values also can be obtained from iterative calculation. Several researchers recently insisted that microbial destruction (log reduction) doesn't follow a linear relationship with temperature [7, 8]. Several non-log-linear models such as Weibull and log-linear + shoulder model have been proposed, and predictive modeling based on the non-log-linear models has been reported [9].

Sang-Soon Kim and Won Choi: These authors contributed equally to this work.

***Corresponding author: Dong-Hyun Kang,** Department of Agricultural Biotechnology, Center for Food and Bioconvergence, and Research Institute for Agricultural and Life Sciences, Seoul National University, Seoul, 08826, Republic of Korea; and Institutes of Green Bio Science & Technology, Seoul National University, Pyeongchang-gun, Gangwon-do, 25354, Republic of Korea, E-mail: kang7820@snu.ac.kr
Sang-Soon Kim: Department of Food Engineering, Dankook University, Cheonan, Chungnam, 31116, Republic of Korea
Won Choi: Department of Landscape Architecture and Rural Systems Engineering, Research Institute for Agriculture and Life Sciences, Seoul National University, Seoul, 08826, Republic of Korea
Sang-Hyun Park: Department of Food Science and Technology, Kongju National University, Yesan, Chungnam, 32439, Republic of Korea

Empirical modeling has long been used not only to predict pathogen inactivation but also to optimize food processing. For example, response surface methodology has been used to optimize treatment conditions in food processing [10, 11]. However, empirical modeling provides no insight into the underlying mechanisms and is unrelated to the physics-based model, and accordingly modeling of food processing has undergone a significant shift from empirical to a physics-based modeling approach [12]. Physics-based modeling including computational simulation enables food engineers to predict precisely temperature distribution and microbial destruction at a specific point in time. Food processing by novel thermal treatments has been of interest, and several researchers analyzed the temperature distribution and microbial inactivation of novel thermal technologies such as microwave, radio-frequency [13–15] including our previous research on ohmic heating [16]. Our previous research [16] focused on the simulation of inactivation of *Escherichia coli* O157:H7 in various amount of orange juice, whereas this study investigated the mathematical modeling of acid-adapted foodborne pathogens in tomato juice. Various software can be used for mathematical modeling such as ANSYS [17–19] and COMSOL [20], and COMSOL software was used in this study.

Tomato-based foods such as tomato juice, tomato paste, and salsa can be processed effectively by ohmic heating because of relatively high electrical conductivity [21]. For example, Palaniappan and Sastry [22] reported that electrical conductivities of tomato juice were ranged ca. 0.5–1.7 S/m, which are proportion to the temperature. Even though juice has traditionally been regarded as safe because of its acidity, several outbreaks have been reported in fruit juices [23, 24]. Foodborne pathogens such as *E. coli* O157:H7, *Salmonella enterica* serovar Typhimurium, and *Listeria monocytogenes* are one of causing agents of the outbreaks, which are known to be adapt to acidic conditions [25]. Heat resistance of these pathogens increased by acid-adaptation, which induces cross-protection against thermal treatments [26, 27]. In this regard, precise prediction of temperature distribution and acid-adapted pathogen inactivation of tomato juice processing by ohmic heating is of importance for processing optimization. Eliminating acid-adapted pathogens during juice processing is very important because they can survive longer than non-acid-adapted pathogens. However, inactivation of acid-adapted pathogens in tomato juice has not yet been analyzed by the numerical simulation, and challenges of this study was how to reflect the increase resistance of pathogen by acid-adaptation.

The objective of the present study was to predict temperature distribution of tomato juice, inactivation trend of acid-adapted foodborne pathogens by ohmic heating using physic-based modeling. High frequency and pulse waveform was used to reduce electrode corrosion rate [28] because electrode corrosion, occur during ohmic heating processing, can be accelerated in acidic food. Significant electrode corrosion would be observed if sine waveform with low frequency was used. Predicted values by simulation was compared with experimental results for validation as previous studies was conducted [29–31].

2 Materials and methods

2.1 Model parameters

The material properties of tomato juice are essential in modeling the ohmic heating. Tomato juice (pH 3.6, 11.8°Brix), used in this study, is composed of water (88.7%), protein (0.5%), fat (0.3%), and carbohydrates (10.5%). The following equations were utilized to predict the density (ρ, kg/m^3), specific heat (C_p, J/kg·K), and thermal conductivity (K, W/m·K) of tomato juice [32];

$$\rho = \sum_{i=1}^{n} \rho_i X_i \tag{1}$$

$$C_p = \sum_{i=1}^{n} C_{pi} X_i \tag{2}$$

$$K = \sum_{i=1}^{n} K_i Y_i \tag{3}$$

where ρ_i, C_{pi}, and K_i are the density, specific heat, and thermal conductivity of the ith component, respectively, in which a food material has n components, and X_i is the weight fraction. Y_i is the volume fraction of the ith component, obtained as follows;

$$Y_i = \frac{X_i/\rho_i}{\sum_{i=1}^{n}(X_i/\rho_i)} \tag{4}$$

The electrode and surrounding materials were made of titanium and acrylic plastic, respectively. The material properties of tomato juice, titanium electrodes, and the acrylic plastic treatment chamber are listed in Table 1. Properties of tomato juice dependent on temperature were used to reflect real situation. The electrical conductivity of tomato juice is identified by voltage and current data [33], and calculated as follows;

$$\sigma = \frac{LI}{AV} \tag{5}$$

where σ is the electrical conductivity (S/m), L is the distance between electrodes (m), I is the current (A), A is the cross-sectional area of the electrode (m^2), and V is the voltage (V).

Voltage, current, and temperature were measured using voltage probe (TPP0101, Tektronix Corp., USA), current clamp (i30s, Fluke, USA) and K-type thermocouples, respectively. Electrical conductivity (mean of three replication) was analyzed with linear expression because it had a linear relationship with temperature ($R^2 > 0.999$, Figure S1).

2.2 Cell suspension preparation and inoculation

E. coli O157:H7 and *Salmonella*, two most causative pathogens in United States, and *L. monocytogenes*, causing premature, miscarriage, and

Table 1: Material properties for simulation.

Material properties	Unit	Tomato juice[a]	Titanium[b]	Acrylic plastic[b]
Density (ρ)	kg/m^3	$-0.03 \times 10^{-2} \times T^2 + 3.37 \times 10^{-2} \times T + 10.61 \times 10^2$	4940	1760
Thermal conductivity (K)	W/(m·K)	$0.06 \times 10^{-4} \times T^2 + 0.17 \times 10^{-2} \times T + 0.54$	7.5	0.1
Specific heat (C_p)	J/(kg·K)	$4.20 \times 10^{-3} \times T^2 + 1.36 \times 10^{-2} \times T + 3.89 \times 10^2$	710	1000
Electrical conductivity (σ)	S/m	$1.76 \times 10^{-2} \times T - 4.70$	74,070	0

[a]Material property equations of tomato juice was calculated based on the composition of tomato juice used in the present study and coefficients to estimate food properties indicated in Appendices of Singh and Heldman (2001) [32].
[b]Imported from COMSOL material library, V4. 3.

stillbirth, were used in this study. Three strains each of *E.* O157:H7 (ATCC 43890, ATCC 35150, and ATCC 43889), *S. typhimurium* (ATCC 19585, ATCC 43971, and DT 104), and *L. monocytogenes* (ATCC 19111, ATCC 19115, and ATCC 15313) were obtained from the bacterial culture collection of the School of Food Science, Seoul National University (Seoul, Republic of Korea). A single colony from a frozen stock was cultivated on tryptic soy agar (TSA; Difco, Becton, Dickinson, Sparks, MD), inoculated into 5 mL of tryptic soy broth (TSB; Difco, Becton, Dickinson, Sparks, MD), incubated at 37 °C for 24 h, collected by centrifugation at 4,000 ×g for 20 min at 4 °C, and washed with 0.2% peptone water (PW; Bacto, Becton, Dickinson, Sparks, MD). The supernatant was decanted, and the final pellets were resuspended in 0.2% PW. Afterward, suspended pellets of the three pathogen strains were combined to comprise a mixed culture cocktail containing approximately equal numbers of cells of each strain of *E. coli* O157:H7 (ca. 10^8 colony forming unit (CFU)/mL), *S. typhimurium* (ca. 10^7 CFU/mL), and *L. monocytogenes* (ca. 10^7 CFU/mL). Pasteurized tomato juice was purchased from a local grocery store (Seoul, Republic of Korea), stored at room temperature (22 ± 1 °C). After opening, tomato juice was stored at refrigerated temperature (4 °C) with cap, and used within two weeks. The mixed-strain cocktail (0.2 mL) was inoculated into 50 mL samples of processed Tomato juice before treatment. Acid-adapted cultures were grown in TSB adjusted to pH 5 with 1 N hydrochloric acid (HCl), and prepared in the same way described above.

2.3 Microbial enumeration

For microbial enumeration, each treated 50 mL sample was immediately transferred into a sterile stomacher bag (Labplas, Inc., Sainte-Julie, Quebec, Canada) containing 100 mL of sterile 0.2% PW and homogenized for 2 min using a stomacher (Easy Mix; AES Chemunex, Rennes, France). After homogenization, 1 mL samples were 10-fold serially diluted with 9 mL of sterile 0.2% PW, and 0.1 mL of stomached samples or diluents were spread plated onto each selective medium. Sorbitol MacConkey (SMAC) agar (Difco), xylose lysine deoxycholate (XLD) agar (Difco), and Oxford agar base (OAB; Difco) with antimicrobial supplement (Bacto Oxford antimicrobial supplement; Difco) were used as selective media for enumeration of *E. coli* O157:H7, *S. typhimurium*, and *L. monocytogenes*, respectively, according to the bacteriological analytical manual (BAM) by USDA. All plates were incubated at 37 °C for 24 to 48 h before counting colonies characteristic of the pathogens. Experiments for pathogen inactivation were replicated three times.

2.4 D- and z-values

For D-value experiments, acid- or non-acid-adapted pathogens were inoculated into 5 mL tomato juice samples in test tubes, previously equilibrate to 45, 50, 55, or 60 °C by immersion in a constant-temperature water bath (BW-10G; Jeio Tech, Seoul, Republic of Korea). Temperature was fixed during treatment, and time was adjusted separately for each temperature. For the D-value experiment, 0.1 mL of treated sample was transferred to 9.9 mL sterile 0.2% PW and enumerated as described in section 2.3. This inactivation experiment was replicated three times and the number of surviving pathogens was plotted on a logarithmic scale as a function of time (min). D_T (min) the time needed to decrease the pathogen population by 90% (1 log) at temperature T (°C), was calculated by plotting surviving microorganisms against time on semi-log coordinates as follows.

$$\log\left(\frac{N}{N_0}\right) = -\frac{t}{D_T} \tag{6}$$

where N_0 = initial pathogen population (CFU/mL), N = pathogen population after treatment (CFU/mL), and t = time (min).

The z-values (°C) were calculated as the negative inverse slope of the linear regression line for the log D-values over the range of heating temperatures tested (Figure S2).

2.5 Ohmic heating setup

The system consisted of a function generator (catalog number 33210A; Agilent Technologies, Palo Alto, CA), a precision power amplifier (catalog number 4510; NF Corp., Yokohama, Japan), a data logger (catalog number 34970A; Agilent Technologies), two rectangular-typed titanium electrodes (0.1 cm thickness, 15.0 cm width, and 6.0 cm height), and an acrylic plastic chamber with inner dimensions (4.2 cm width, 15.2 cm length, and 6.0 cm height) and thickness of 0.5 cm. The schematic diagram of system and geometry of heating chamber are described in the previous study [34]. The electrodes were installed in the ohmic heating chamber, and the distance between the two electrodes was set up to be 4 cm. Each 50 mL tomato juice sample, inoculated with a mixed-culture cocktail, was subjected to 25 V_{rms}/cm ohmic heating (1 kHz, pulse waveform, alternating current (AC), 0.05 duty ratio) for 0, 30, 50, 60, 65, 70, and 75 s considering preliminary experiments. The high frequency (1 kHz) and pulse waveform were used to prevent electrode corrosion as reported by previous researcher [28].

2.6 Mathematical model

Simulation for ohmic heating treatment was conducted using COMSOL software (Version 4.3, COMSOL Inc., Palo Alto, CA) based on the finite element method (FEM), which is widely used to solve the problems of engineering and mathematical models along with BEM and DQM [35].

Simulated results were compared with experimental results at points 1, 2, and 3 for validation (Figure 1). Point 1 was selected because it is the geometrical center of the chamber. Point 2 and 3 were selected as edge and side of chamber, respectively.

2.6.1 Governing equation for electric field: The Laplace equation defining the electric field in an ohmic heater was given by:

$$\nabla \cdot (\sigma(T)\,\nabla V) = 0 \tag{7}$$

Boundary and initial conditions for ohmic conductor were given by:

Electrode with a ground : $V = 0$
Electrode with an electric potential : $V = V_0$
Electrical insulation at the walls : $\mathbf{n}(\sigma(T)\,\nabla V) = 0$

where $\mathbf{n}$ is the unit vector perpendicular to the boundary.

2.6.2 Governing equation for heat balance: The governing equation including heat generation and transfer is defined by:

$$\rho C_p \frac{\partial T}{\partial t} = \nabla \cdot (k\,\nabla T) + Q - \rho C_p \mathbf{u} \cdot \nabla T \tag{8}$$

where $\mathbf{u}$ is the velocity (m/s), and Q is the heat source (W/m^3) generated by ohmic heater. The heat sources produced by ohmic heater can be calculated by the following equation.

$$Q = \sigma(T)|\nabla V|^2 \tag{9}$$

Boundary condition for external natural convection on the surfaces of chamber is given by:

$$\mathrm{n} \cdot (k\,\nabla T) = h(T_{ext} - T) \tag{10}$$

where h is the convective heat transfer coefficient (W/m^2·K), and T_{ext} is the external environment temperature (K). The heat transfer coefficient for natural convection can be changed depending on the geometrical configuration (vertical or horizontal face). The coefficient is also the function of the length (area/perimeter, m), internal and external temperatures, thermal conductivity, and so on. For most engineering purposes, the COMSOL software (v 4.3, CA) provides built-in functions for the heat transfer coefficient. Thus, the heat transfer coefficient was automatically calculated by the software with the initial temperature of 22 °C (external temperature).

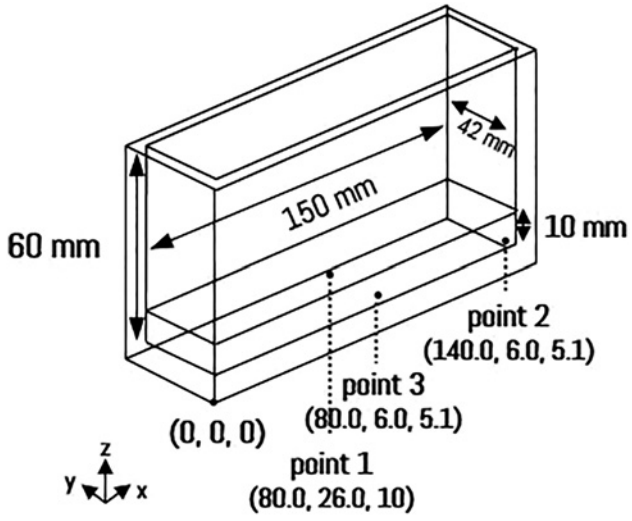

Figure 1: Dimensions and designation of points 1, 2, and 3 of ohmic heating chamber.

2.6.3 Governing equation for incompressible laminar flow: If the flow condition is in an incompressible state with respect to time and space, the governing equations using Cartesian coordinates can be described by the following laminar flow model, which are part of Navier–Stokes equations for incompressible flow. Boussinesq approximation was considered, which means that the only affect of density is in the gravitational term (the buoyancy force).

$$\rho \frac{\partial \mathbf{u}}{\partial t} + \rho(\mathbf{u} \cdot \nabla)\mathbf{u} = \nabla \cdot \left[-p\mathbf{I} + \mu\left(\nabla \mathbf{u} + (\nabla \mathbf{u})^{tr}\right)\right] + \rho g \tag{11}$$

$$\rho\,\nabla \cdot (\mathbf{u}) = 0 \tag{12}$$

where p is the pressure (Pa), μ is the dynamic viscosity (Pa·s), $\mathbf{I}$ is the identity vector, $\boldsymbol{g}$ is the gravitational acceleration (9.8 m/s^2), and superscript *tr* is the transpose of a matrix.

The dynamic viscosity and density of fluid are changed depending on the temperature and initial condition of velocity was set to be zero. The density variation drives the buoyant flow.

2.6.4 Equation for pathogen inactivation: Transport of diluted species module in chemical species transport was used to simulate pathogen inactivation. Initial population of *E. coli* O157:H7, *S. typhimruium*, and *L. monocytogenes* were considered as 5.85, 5.46, and 6.04 CFU/mL, respectively, based on the experimental results. Pathogens were considered to be homogenously distributed along the juice sample. Following first-order reaction equation was assumed to be an appropriate model to predict the inactivation of foodborne pathogens based on experimental D-value results;

$$\frac{\partial c}{\partial t} = k_T c \tag{13}$$

where c is the concentration (CFU/mL·m^3), and k_T is the reaction rate constant (1/s).

The relationship between the reaction rate constant and the decimal reduction time is defined as follows:

$$k_T = \frac{2.303}{D_T} \tag{14}$$

2.7 Simulation setup

A 3 dimensional (3D) geometry of the ohmic heating chamber created by AutoCAD 2010 software (Autodesk, Inc., San Rafael, CA) was imported into COMSOL software. The domains were discretized by free tetrahedral meshes (which was optimized in this study), resulting in 54,034 elements, using the advanced front method (AFM). The domains were discretized by free tetrahedral meshes using AFM to increase convergence rate. The averaged mesh quality (Q) was kept at 0.7224 throughout the domains.

$$Q = \frac{4\sqrt{3}A}{h_1^2 + h_2^2 + h_3^2} \tag{15}$$

where A is the area of triangle, and h_1, h_2, and h_3 are the side lengths of the triangle.

Fluid dynamics and heat transfer of solution, and pathogen inactivation during batch type ohmic heating were setup through the software. The partial differential equations (PDEs) to govern

the phenomena were simultaneously solved based on the FEM, and a parallel direct sparse solver (PARDISO), optimized for the numerical simulation and fast, was selected. The simulation was run using a personal server-level computer (Intel Xeon CPU E-mail: X5690@4.00GHz (2 Processors), 32 GB@1,600 MHz RAM on a Windows 7 64-bit operating system). Heating and pathogen inactivation rates were identified meticulously at three points inside the chamber (Figure 2). Experimental results were compared with simulated values at these three points for the verification of simulation model.

2.8 Statistical analysis

D and z values were analyzed by the analysis of variance procedure of the Statistical Analysis System (SAS 9.3, SAS Institute, Cary, NC) and mean values were separated using widely used Tukey's honestly significant difference (HSD) test. Simulated and experimental populations of pathogens were analyzed by the *t*-test because just two groups were compared. Significant differences between experimental and simulated results were determined at a significance level of $p = 0.05$.

3 Results and discussion

3.1 Thermal resistance of regular (non-acid-adapted) pathogens

Thermal resistance of foodborne pathogens at a constant temperature in tomato juice differed for each pathogen (Table 2). Specifically, D-values of *E. coli* O157:H7 were higher than those of *S. typhimurium* or *L. monocytogenes* for every isothermal temperature investigated in the present study. These results indicated that *E. coli* O157:H7 had the highest thermal resistance to the ohmic heating under the treatment conditions of our study. Similar results were reported by Mazzotta [27], who investigated the heat resistance of *E. coli* O157:H7, *S. enterica (serotypes Typhimurium, Enteritidis, Gaminara, Rubislaw, and Hartford)*, and *L. monocytogenes* in fruit juices, and identified that *E. coli* O157:H7 had the highest heat resistance among the investigated pathogens. For example, D-values at 60 °C of non-acid-adapted *E. coli* O157:H7, *S. enterica*, and *L. monocytogenes* in orange juice were 1.1 ± 0.35, 0.21 ± 0.10, and 0.43 ± 0.06 min, respectively. Gabriel and Nakano [36] also reported that D-value of *E. coli* O157:H7 was the highest followed by *L. monocytogenes* and *S. typhimurium* when pathogens were subjected to 55 °C apple juice. Introducing heat resistance data in a buffer experiments to the food processing simulation would result in the significant difference because the resistances in the buffer and the food matrix are considerably different due to acidity, nutritional content, and so on [37]. Moreover, Syamaladevi et al. [38] reported that water activity (a_w) in low-moisture food has been recognized as the primary factors influencing the heat resistance of pathogen. Therefore, computational

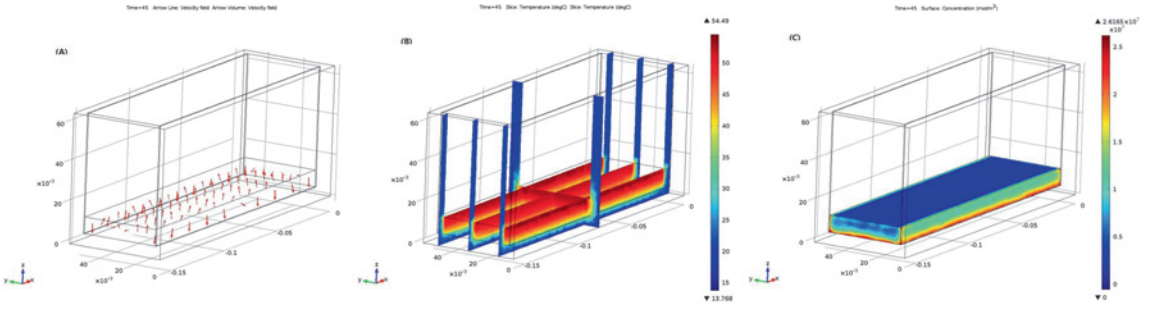

Figure 2: Simulated velocity (A) and temperature distribution (B) after 45 s ohmic heating treatment (25 V/cm), and concentration of *E. coli* O157:H7 (C) after the treatment.

Table 2: D-values of regular (non-acid-adapted) pathogens[a,b].

Bacterium[c]	D-value (min)			
	45 °C	50 °C	55 °C	60 °C
E	14.90 ± 2.58^{Aa}	8.60 ± 0.83^{Ab}	1.55 ± 0.75^{Ac}	0.26 ± 0.16^{Ac}
S	12.87 ± 1.47^{Aa}	4.09 ± 0.87^{Bb}	1.02 ± 0.19^{Ac}	0.14 ± 0.07^{Ac}
L	11.56 ± 1.54^{Aa}	1.78 ± 0.61^{Cb}	0.60 ± 0.11^{Ab}	0.15 ± 0.06^{Ab}

Mean values ± standard deviation (replicated 3 times).

[a] Values in the same column followed by the same uppercase letter are not significantly different ($p > 0.05$).

[b] Values in the same row followed by the same lowercase letter are not significantly different for D-values ($p > 0.05$).

[c] E: *E. coli* O157:H7, S: *S. typhimurium*, L: *L. monocytogenes*.

simulation was conducted by combining physical-based numerical approaches using COMSOL software with experimental models of D-values and electrical conductivity measured and calculated in the present study (Table 1). First-order kinetic based on D-values was used in this study, but further study is needed to combining non-log linear models with physical-based approaches.

3.2 Computational simulation of ohmic heating with regular (non-acid-adapted) pathogen

Tomato juice processing by ohmic heating with rectangular heater was analyzed through a mathematical model. Even though various type of heater can be used for ohmic heating, rectangular heater has been widely used for batch type system [16], [21], [25]. Velocity and temperature distribution of tomato juice, and concentration of *E. coli* O157:H7 after 45 s treatment, at which the non-uniformity was remarkable, were represented to help understanding the nature of processing (Figure 2). The temperature at the center of the chamber was relatively higher than other location because heat losses occurred from the heating chamber to the outside by natural convection [39]. In the beginning, the convection caused relatively hot fluids at the center to rise, and this phenomenon contributed to upward-moving streamlines at the center of the ohmic heating chamber (Figure 2A). In this regard, most of the upper part of tomato juice sample showed a red color indicating a temperature of around 50 °C while the lower part of tomato juice displayed a yellow color corresponding to temperatures around 40 °C after 45 s treatment (Figure 2B). Marra et al. [1] also reported that more cold areas were observed at the sample surface in a closed cylindrical ohmic heating cell, and Varghese et al. [40] indicated that these colder external shells were critical areas to be monitored. Fryer et al. [41] indicated that for low-viscosity systems, where fluid viscosity is comparable to that of water, it is possible to assume that the liquid temperature is uniform. Even though the viscosity of normally processed tomato juice is around 13.0 cP [42], the processing time was much shorter than that in Fryer et al.'s study, and then the convection inside of the chamber in the present study was not enough to ensure heating uniformity of tomato juice. Because the cold point was observed in the lower part of the ohmic heating chamber, it is predicted that some pathogens still can survive in these areas of the chamber at 45 s (Figure 2C), even though all pathogens were inactivated elsewhere. Non-uniformity was more severe for larger quantity of samples when different amount of orange juice samples were subjected to ohmic heating [16]. In this regard, uniformity of larger quantity of tomato juice samples should be considered when ohmic heating is applied in the juice industry.

After executing computational simulation, it is needed to verify that the developed model values accurately predict observed values. Heating rate and inactivation of pathogens by computational simulation were compared with experimental results for the verification. The heating rates of simulation were similar to experimental results within an error range of 4.5 °C at points 1, 2, and 3 (Figure 3). Heated samples, which has lower density than around, rose due to buoyancy. This phenomenon would actively progress as treatment time increase. It is assumed that this natural convection resulting in temperature difference inside the chamber. The modeled heating rates had a more linear shape than experimental results, which represented exponential shape. It is well known that temperature increase trend by ohmic heating has exponential shape because electrical conductivity is proportion to temperature [22]. Electrical conductivity, also proportion to temperature in the present study, was considered for modeling. Even though maximum error value at 3 points was 4.5 °C, that at point 2 and over 45 °C (which contribute to the pathogen inactivation) was 2.26 °C (Table S1). In this regard, the simulated inactivation value was similar with experimental results and it was assumed that validation of simulation was conducted by comparing the temperature. In the cases of pathogen inactivation trends, experimental results were much closer to simulated results at point 2 than at points 1 or 3 (Figure 4). The simulated results at point 2 were not exactly identical with experimental results of which were obtained from microbial count of the whole

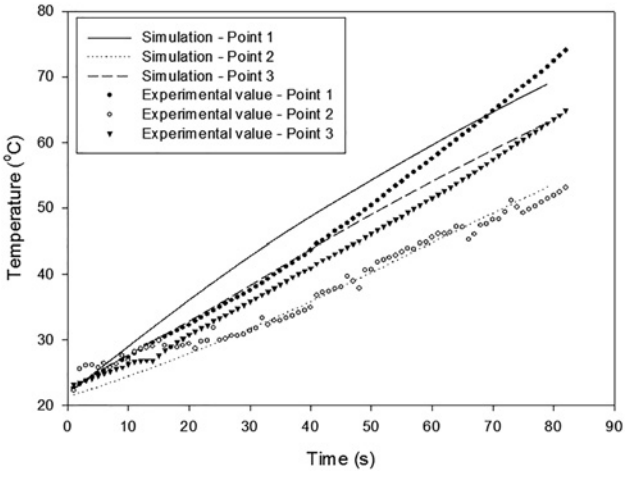

Figure 3: Comparison of the simulated and experimental temperatures of ohmic heated tomato juice at points 1, 2, and 3.

sample. It was not possible to sample the exact portion at specific position. Therefore, three points were designated to investigate which point is the most similar with overall inactivation trend. Moreover, pathogens were assumed to be stay at the specific point even though they move to the other point and subject to the other temperature at real situation. Further study should be conducted considering the movement of pathogens.

At certain treatment time, more than 5 log CFU/mL pathogen can exist at point 2 while only less than 1 log CFU/mL can survive at point 1 or 3. Therefore, temperature at point which have lower heating rate (point 2 in the present study) leads the overall microbial inactivation trend. Moreover, only temperature over than 45 °C contribute the pathogen inactivation. Considering these factors, actual error range (at point 2 and over 45 °C) is within 2.26 °C (Table S1) because lower temperature would not inactivate the pathogen. These results indicate that the point 2 must be selected as a biological validation spot. Because heat resistances were differed for the type of pathogen, the times needed to inactivate pathogens by ohmic heating were different for each pathogen. When pathogen inactivation at point 2 was simulated, 76.3, 70.9, and 68.3 s would be needed to inactivate *E. coli* O157:H7, *S. typhimurium*, and *L. monocytogenes*, respectively, to below the detection limit. These simulated treatment intervals were very similar to experimental results, which indicated that 75, 70, and 70 s were needed to inactivate *E. coli* O157:H7, *S. typhimurium*, and *L. monocytogenes*, respectively, to below the detection limit. From the results above, it was verified that developed simulation model can predict the temperature increase and microbial inactivation without significant difference with experimental results. The results are consistent with previous research investigations reporting that physics-based modeling can predict the temperature distribution and microbial inactivation precisely [13, 14].

3.3 Computational simulation of ohmic heating with acid-adapted pathogen

After verification of the model, it was investigated whether the developed simulation model can predict the inactivation of acid-adapted pathogens. Heat resistance of the acid-adapted pathogens increased compared to non-acid-adapted pathogens (Tables 2 and 3). D-values increased considerably at 55 °C and 60 °C for acid-adapted *E. coli* O157:H7, whereas for acid-adapted *S. typhimurium* and *L. monocytogenes*, D-values significantly increased between 45 and 50 °C compared to non-acid-adapted cells. Acid-adaption increase lethal temperature of pathogens. Because the lethal temperature of *E. coli* O157:H7 was higher than those of *S. typhimurium* and *L. monocytogenes* before acid-adaptation, it seems that the acid-adaptation affect the D-values of *E. coli* O157:H7 at higher temperature than those of *S. typhimurium* and *L. monocytogenes*. In this regard, the z-value of acid-adapted *E. coli* O157:H7 was significantly higher ($p < 0.05$) than that of non-acid-adapted cells at the range of 45–60 °C (Table 4). On the other hand, z-values of acid-adapted *S. typhimurium* and *L. monocytogenes* were not significantly different from ($p > 0.05$) than those of non-acid-adapted *S. typhimurium* and *L. monocytogenes*, respectively, at the range of 45–60 °C. Mazzotta [27] also reported that D-values of *E. coli* O157:H7, *S. typhimurium*, and *L. monocytogenes* increased after acid-adaptation in apple, orange, and white grape juices, and z-values increased or decreased depending on the type of pathogen and juice. Altered D-values by acid-adaptation were adopted to computational simulation to predict inactivation trend of acid-adapted pathogens by ohmic heating, and point 2 was used to predict the inactivation trend considering the results of section 3.3 (Table 5). Acid-adaption did not affect the electrical conductivity of the tomato juice. Acid-adapted cultures were grown in TSB adjusted to pH 5 with 1 N HCl, and collected by

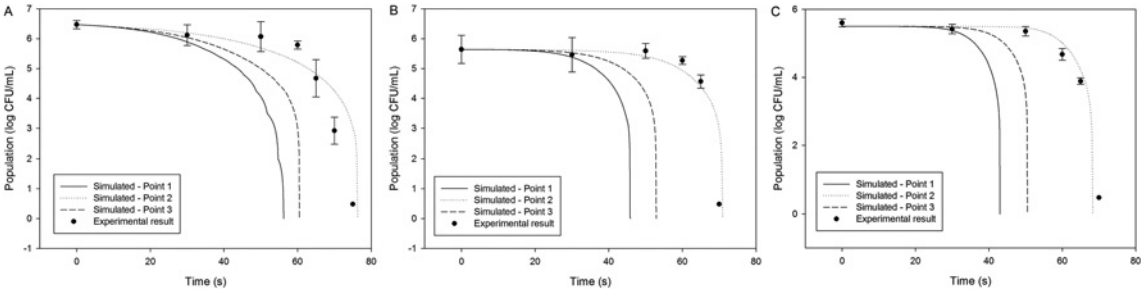

Figure 4: Comparison of the simulated and experimental population (log CFU/ml) of *E. coli* O157:H7 (A), *S. Typhimurium* (B), and *L. monocytogenes* (C) in tomato juice subjected to ohmic heating. Experimental results were represented as the mean ± standard deviation ($n = 3$).

Table 3: Altered D-values of pathogens by acid-adaptation[a,b].

Bacterium[c]	D-value (min)			
	45 °C	50 °C	55 °C	60 °C
E	18.89 ± 5.33^{Aa}	10.18 ± 2.78^{Abc}	4.73 ± 2.49^{Abc}	0.81 ± 0.31^{Ac}
S	23.04 ± 7.28^{Aa}	6.52 ± 2.01^{ABb}	1.04 ± 0.21^{Bb}	0.18 ± 0.07^{Bb}
L	21.50 ± 4.75^{Aa}	4.02 ± 1.61^{Bb}	0.79 ± 0.32^{Bb}	0.22 ± 0.07^{Bb}

Mean values ± standard deviation (replicated 3 times).
[a] Values in the same column followed by the same uppercase letter are not significantly different ($p > 0.05$).
[b] Values in the same row followed by the same lowercase letter are not significantly different for D-values ($p > 0.05$).
[c] E: *E. coli* O157:H7, S: *S. typhimurium*, L: *L. monocytogenes*.

centrifugation, and washed with 0.2% PW. Therefore, conditions for collated cultures are identical for acid-adapted and non-acid-adapted pathogens. Further study is needed using the acid-adapted or acid-shocked pathogens at more severe conditions (pH 3–4) considering that the pH of juice products are 3–4. Koutsoumanis et al. [43] reported that a mild acid shock at pH 5.0, 5.5, or 6.0 resulted in an increase in the pathogen resistance to acid conditions (pH 3.5) whereas acid shock at pH 4.0, 4.5, and 7.0 had no significant effect, but the results would be different for the heat resistance.

Table 4: z-values of regular (non-acid-adapted) and acid-adapted pathogens[a,b].

Bacterium[c]	Regular	Acid-adpated
E	8.13 ± 1.21^{Aa}	11.34 ± 2.17^{Ab}
S	7.68 ± 0.91^{Aa}	7.01 ± 0.52^{Ba}
L	8.13 ± 0.50^{Aa}	7.42 ± 0.20^{Ba}

Mean values ± standard deviation (replicated 3 times).
[a] Values in the same column followed by the same uppercase letter are not significantly different ($p > 0.05$).
[b] Values in the same row followed by the same lowercase letter are not significantly different for D-values ($p > 0.05$).
[c] E: *E. coli* O157:H7, S: *S. typhimurium*, L: *L. monocytogenes*.

Experimental log reductions were higher than computationally predicted values, which is consistent with previous studies [44, 45]. Xu et al. [45] reported that experimental log reductions by radio-frequency pasteurization of *Enterococcus faecium* were higher than those of predicted model, and pointed out that an unavoidable delay may have occurred removing treated samples from the processing container. It was postulated that not only the delay but also the mixing effect during the sampling stage would contribute to increasing experimental log reduction. In particular, the delay and/or the mixing effect would have more significant effect on the inactivation of acid-adapted pathogens due to the increased resistance compared to the non-acid-adapted pathogens. Despite these unavoidable experimental limitations, the differences between simulated and experimental data were not significant under any treatment conditions ($p > 0.05$) when analyzed by the Satterthwaite *t*-test considering inequality of variance. The results indicated that computational simulation not only reflect the increased heat resistance by acid-adaptation but also be utilized more extensively by replacing the heat resistance value (D-value) considering the environmental conditions of pathogens. Therefore, computational model can be utilized effectively to predict the pathogen inactivation trend of which the heat

Table 5: Simulated and experimental populations (log CFU/mL) of pathogens after acid-adaptation.

Treatment Time (s)	*E. coli* O157:H7[b]		*S. Typhimurium*[b]		*L. monocytogenes*[b]	
	Sim[a]	Exp[a]	Sim[a]	Exp[a]	Sim[a]	Exp[a]
0	5.85^{A}	5.85 ± 0.53^{A}	5.46^{A}	5.46 ± 0.19^{A}	6.04^{A}	6.04 ± 0.12^{A}
30	5.82^{A}	5.71 ± 0.67^{A}	5.46^{A}	5.55 ± 0.14^{A}	6.04^{A}	5.98 ± 0.05^{A}
50	5.69^{A}	5.65 ± 0.88^{A}	5.43^{A}	5.68 ± 0.13^{A}	5.98^{A}	5.90 ± 0.16^{A}
60	5.43^{A}	4.54 ± 0.87^{A}	5.26^{A}	4.95 ± 0.17^{A}	5.72^{A}	5.64 ± 0.09^{A}
65	5.17^{A}	4.68 ± 0.61^{A}	4.94^{A}	4.98 ± 0.46^{A}	5.30^{A}	5.00 ± 0.30^{A}
70	4.73^{A}	4.55 ± 0.81^{A}	4.26^{A}	3.97 ± 0.88^{A}	4.39^{A}	3.46 ± 1.04^{A}
75	3.90^{A}	2.70 ± 1.08^{A}	<0.48^{A}	<0.48^{A}	<0.48^{A}	0.91 ± 0.75^{A}

[a] Sim: Simulated results at point 2, Exp: Experimental results (Mean values ± standard deviation, replicated 3 times).
[b] Values in the same row that are followed by the same letter are not significantly different for each pathogen ($p > 0.05$).

resistance increased abnormally due to the climate change and cross-protection.

4 Conclusion

Ohmic heating processing of tomato juice, including the prediction of acid-adapted pathogen inactivation, was mathematically analyzed in the present study. Electrical, thermo-physical properties of materials and thermal resistance values of pathogens were reflected in the mathematical modeling. In the simulation, upward-moving streamlines were observed at the center of the chamber, which contributed to the overall temperature distribution of ohmic heating. Because simulated temperature at the lower part of the chamber was lower than that of the higher part, pathogens can survive longer at the bottom or corner of the treatment chamber than those of higher part. Three points were designated to understand temperature and biological states at each location more meticulously. Verification, comparing simulated values with experimental results, was accomplished at the three points. Significant differences were not observed between experimental acid-adapted pathogen reductions and simulated values ($p > 0.05$), which means the errors are within the range each other. Limited points were simulated and validated in this study, but this is the first attempt to predict the acid-adapted pathogen inactivation by computer simulation. Further study is needed to simulated pathogen inactivation adapted to various environmental conditions. From the results in this study, it is recommended to utilize the mathematical model approach to reduce time and labor optimizing processing conditions. After that, confirmation experiment is needed to ensure microbiological safe. This model could be helpful for juice processors desiring 5-log reductions of target organisms because processing conditions should be adjusted for the environmental conditions affecting heat resistance of pathogens.

Author contribution: All the authors have accepted responsibility for the entire content of this submitted manuscript and approved submission.

Research funding: This work was also supported by a National Research Foundation of Korea (NRF) grant funded by the South Korean government (grant NRF-2018R1A2B2008825). This work was also supported by Creative-Pioneering Researchers Program through Seoul National University (SNU).

Employment or leadership: None declared.

Honorarium: None declared.

Conflict of interest statement: The authors declare no conflicts of interest regarding this article.

Nomenclature

Symbol	Parameter	Units	Note
ρ	Density	kg/m^3	Table 1
C_p	Specific heat	J/kg·K	Table 1
K	Thermal conductivity	W/m·K	Table 1
σ	Electrical conductivity	S/m	Table 1
D_T	Decimal reduction time	min	Tables 2 and 3
z-value	Death rate change	°C	Tables 2 and 3
V_o	Applied voltage	V	100
T_o	Initial temperature	K	295.15
L	Distance between electrodes	m	Equation 5
I	Current	A	Equation 5
A	Cross-sectional area of electrode	m^2	Equation 5
V	Voltage	V	Equation 5
N	Pathogen population	CFU/mL	Equation 6
N_o	Initial pathogen population	CFU/mL	Equation 6
t	Treatment time	min	Equation 6
u	Velocity	m/s	Equation 8
Q	Heat generation	W/m^3	Equation 9
h	Convective heat transfer coefficient	W/m^2·K	Equation 10
μ	Dynamic viscosity	Pa·s	Equation 11
p	Pressure	Pa	Equation 11
g	Gravitational acceleration	m/s^2	Equation 11

References

1. Marra F, Zell M, Lyng J, Morgan D, Cronin D. Analysis of heat transfer during ohmic processing of a solid food. J Food Eng 2009; 91:56–63. https://doi.org/10.1016/j.jfoodeng.2008.08.015.
2. Leizerson S, Shimoni E. Effect of ultrahigh-temperature continuous ohmic heating treatment on fresh orange juice. J Agr Food Chem 2005;53:3519–24. https://doi.org/10.1021/jf0481204.
3. Leizerson S, Shimoni E. Stability and sensory shelf life of orange juice pasteurized by continuous ohmic heating. J Agri Food Chem 2005;53:4012–8. https://doi.org/10.1021/jf047857q.
4. Tian X, Yu Q, Wu W, Dai R. Inactivation of microorganisms in foods by ohmic heating: a review. J Food Protect 2018;81:1093–107. https://doi.org/10.1021/jf0481204.
5. Juneja VK. Predictive model for the combined effect of temperature, sodium lactate, and sodium diacetate on the heat resistance of *Listeria monocytogenes* in beef. J Food Protect 2003;66:804–11. https://doi.org/10.4315/0362-028x-66.5.804.
6. Juneja VK, Eblen BS. Predictive thermal inactivation model for *Listeria monocytogenes* with temperature, pH, NaCl, and sodium pyrophosphate as controlling factors. J Food Prot 1999; 62:986–93. https://doi.org/10.4315/0362-028x-62.9.986.
7. Geeraerd A, Valdramidis V, Van Impe J. GInaFiT, a freeware tool to assess non-log-linear microbial survivor curves. Int J Food Microbiol 2005;102:95–105. https://doi.org/10.1016/j.ijfoodmicro.2004.11.038.

8. Song WJ, Kang DH. Influence of water activity on inactivation of *Escherichia coli* O157: H7, *Salmonella* Typhimurium and *Listeria monocytogenes* in peanut butter by microwave heating. Food Microbiol 2016;60:104–11. https://doi.org/10.1016/j.fm.2016.06.010.
9. Ha JW, Kang DH. Inactivation kinetics of *Escherichia coli* O157: H7, *Salmonella enterica* Serovar Typhimurium, and *Listeria monocytogenes* in ready-to-eat sliced ham by near-infrared heating at different radiation intensities. J Food Protect 2014;77:1224–8. https://doi.org/10.4315/0362-028X.JFP-13-561.
10. Kim SS, Jo Y, Kang DH. Combined inhibitory effect of milk fat and lactose for inactivation of foodborne pathogens by ohmic heating. LWT-Food Sci Technol 2017;86:159–65. https://doi.org/10.1016/j.lwt.2017.07.043.
11. Song M, Kim H, Rhee M. Optimization of heat and relative humidity conditions to reduce *Escherichia coli* O157: H7 contamination and maximize the germination of radish seeds. Food Microbiol 2016;56:14–20. https://doi.org/10.1016/j.fm.2015.12.001.
12. Saguy IS. Challenges and opportunities in food engineering: modeling, virtualization, open innovation and social responsibility. J Food Eng 2016;176:2–8. https://doi.org/10.1016/j.jfoodeng.2015.07.012.
13. Hong YK, Huang L, Yoon WB, Liu F, Tang J. Mathematical modeling and Monte Carlo simulation of thermal inactivation of non-proteolytic *Clostridium botulinum* spores during continuous microwave-assisted pasteurization. J Food Eng 2016;190:61–71. https://doi.org/10.1016/j.jfoodeng.2016.06.012.
14. Jiao Y, Tang J, Wang S. A new strategy to improve heating uniformity of low moisture foods in radio frequency treatment for pathogen control. J Food Eng 2014;141:128–38. https://doi.org/10.1016/j.jfoodeng.2014.05.022.
15. Nguyen LT, Choi W, Lee SH, Jun S. Exploring the heating patterns of multiphase foods in a continuous flow, simultaneous microwave and ohmic combination heater. J Food Eng 2013;116:65–71. https://doi.org/10.1016/j.jfoodeng.2012.11.011.
16. Choi W, Kim SS, Park SH, Ahn JB, Kang DH. Numerical analysis of rectangular type batch ohmic heater to identify the cold point. Food Sci Nutr 2020;8:648–58. https://doi.org/10.1002/fsn3.1353.
17. Abadi AME, Sadi M, Farzaneh-Gord M, Ahmadi MH, Kumar R, Chau K. A numerical and experimental study on the energy efficiency of a regenerative heat and mass exchanger utilizing the counter-flow Maisotsenko cycle. Eng Appl Comp Fluid 2020;14:1–12. https://doi.org/10.1080/19942060.2019.1617193.
18. Farzaneh-Gord M, Faramarzi M, Ahmadi MH, Sadi M, Shamshirband S, Mosavi A, et al. Numerical simulation of pressure pulsation effects of a snubber in a CNG station for increasing measurement accuracy. Eng Appl Comp Fluid 2019;13:642–63. https://doi.org/10.1080/19942060.2019.1624197.
19. Ramezanizadeh M, Nazari MA, Ahmadi MH, Chau K. Experimental and numerical analysis of a nanofluidic thermosiphon heat exchanger. Eng Appl Comp Fluid 2019;13:40–7. https://doi.org/10.1080/19942060.2018.1518272.
20. Park SH, Choi W, Kim SS, Kang DH. CFD simulation for designing a chlorine gaseous sanitizer treatment system. Food Bioprod Process 2019;117:388–95. https://doi.org/10.1016/j.fbp.2019.08.008.
21. Lee SY, Sagong HG, Ryu S, Kang DH. Effect of continuous ohmic heating to inactivate *Escherichia coli* O157: H7, *Salmonella* Typhimurium and *Listeria monocytogenes* in orange juice and tomato juice. J Appl Microbiol 2013;112:723–31. https://doi.org/10.1111/j.1365-2672.2012.05247.x.
22. Palaniappan S, Sastry SK. Electrical conductivity of selected juices: influences of temperature, solids content, applied voltage, and particle size 1. J Food Process Eng 1991;14:247–60. https://doi.org/10.1111/j.1745-4530.1991.tb00135.x.
23. Cook KA, Dobbs TE, Hlady WG, Wells JG, Barrett TJ, Puhr ND, et al. Outbreak of *Salmonella* serotype Hartford infections associated with unpasteurized orange juice. JAMA 1998;280:1504–9. https://doi.org/10.1001/jama.280.17.1504.
24. Enache E, Chen Y. Survival of *Escherichia coli* O157: H7, *Salmonella*, and *Listeria monocytogenes* in cranberry juice concentrates at different Brix levels. J Food Protect 2007;70:2072–7. https://doi.org/10.4315/0362-028X-70.9.2072.
25. Lee JY, Kim SS, Kang DH. Effect of pH for inactivation of *Escherichia coli* O157: H7, *Salmonella* Typhimurium and *Listeria monocytogenes* in orange juice by ohmic heating. LWT-Food Sci Technol 2015;62:83–8. https://doi.org/10.1016/j.lwt.2015.01.020.
26. Álvarez-Ordóñez A, Fernández A, López M, Arenas R, Bernardo A. Modifications in membrane fatty acid composition of *Salmonella* typhimurium in response to growth conditions and their effect on heat resistance. Int J Food Microbiol 2008;123:212–9. https://doi.org/10.1016/j.ijfoodmicro.2008.01.015.
27. Mazzotta AS. Thermal inactivation of stationary-phase and acid-adapted *Escherichia coli* O157: H7, *Salmonella*, and *Listeria monocytogenes* in fruit juices. J Food Protect 2001;64:315–20. https://doi.org/10.4315/0362-028x-64.3.315.
28. Samaranayake CP, Sastry SK, Zhang H. Pulsed ohmic heating–a novel technique for minimization of electrochemical reactions during processing. J Food Sci 2005;70:e460–5. https://doi.org/10.1111/j.1365-2621.2005.tb11515.x.
29. Baghban A, Sasanipour J, Pourfayz F, Ahmadi MH, Kasaeian A, Chamkha AJ, et al. Towards experimental and modelling study of heat transfer performance of water-SiO2 nanofluid in quadrangular cross-section channels. Eng Appl Comp Fluid 2019;13:453–69. https://doi.org/10.1080/19942060.2019.1599428.
30. Jakubowski M, Stachnik M, Sterczynska M, Matysko R, Piepiorka-Stepuk J, Dowgiallo A, et al. CFD analysis of primary and secondary flows and PIV measurement in whirlpool and whirlpool kettle with pulsatile filling: analysis of the flow in a swirl separator. J Food Eng 2019;258:27–33. https://doi.org/10.1016/j.jfoodeng.2019.04.003.
31. Stachnik M, Jakubowski M. Multiphase model of flow and separation phases in a whirlpool: advanced simulation and phenomena visualization approach. J Food Eng 2020;274:109846. https://doi.org/10.1016/j.jfoodeng.2019.109846.
32. Singh RP, Heldman DR. Introduction to food engineering. Gulf Professional Publishing; 2001.
33. Palaniappan S, Sastry SK. Electrical conductivities of selected solid foods during ohmic heating 1. J Food Process Eng 1991;14:221–36. https://doi.org/10.1111/j.1745-4530.1991.tb00093.x.
34. Kim SS, Kang DH. Combination treatment of ohmic heating with various essential oil components for inactivation of food-borne pathogens in buffered peptone water and salsa. Food Control 2017;80:29–36. https://doi.org/10.1016/j.foodcont.2017.04.001.

35. Ghalandari M, Shamshirband S, Mosavi A, Chau K. Flutter speed estimation using presented differential quadrature method formulation. Eng Appl Comp Fluid 2019;13:804–10. https://doi.org/10.1080/19942060.2019.1627676.
36. Gabriel AA, Nakano H. Inactivation of *Salmonella, E. coli* and *Listeria monocytogenes* in phosphate-buffered saline and apple juice by ultraviolet and heat treatments. Food Control 2009;20:443–6. https://doi.org/10.1016/j.foodcont.2008.08.008.
37. Kim SS, Kang DH. Effect of milk fat content on the performance of ohmic heating for inactivation of *Escherichia coli* O157: H7, *Salmonella enterica* Serovar Typhimurium and *Listeria monocytogenes*. J Appl Microbiol 2015;119:475–86. https://doi.org/10.1111/jam.12867.
38. Syamaladevi RM, Tang J, Villa-Rojas R, Sabani S, Carter B, Campbell G. Influence of water activity on thermal resistance of microorganisms in low-moisture foods: A review. Compr Rev Food Sci Food Safety 2016;15:353–70. https://doi.org/10.1111/1541-4337.12190.
39. Kim SS, Sung HJ, Kwak HS, Joo IS, Lee JS, Ko G, et al. Effect of power levels on inactivation of *Escherichia coli* O157: H7, *Salmonella* Typhimurium, and *Listeria monocytogenes* in tomato paste using 915-megahertz microwave and ohmic heating. J Food Protect 2016;79:1616–22. https://doi.org/10.4315/0362-028X.JFP-16-044.
40. Varghese KS, Pandey M, Radhakrishna K, Bawa A. Technology, applications and modelling of ohmic heating: a review. J Food Sci Technol 2014;51:2304–17. https://doi.org/10.1007/s13197-012-0710-3.
41. Fryer P, De Alwis A, Koury E, Stapley A, Zhang L. Ohmic processing of solid-liquid mixtures: heat generation and convection effects. J Food Eng 1993;18:101–25. https://doi.org/10.1111/j.1745-4530.1998.tb00463.x.
42. Kaur C, George B, Deepa N, Jaggi S, Kappor HC. Viscosity and quality of tomato juice as affected by processing methods. J Food Quality 2007;30:864–77. https://doi.org/10.1111/j.1745-4557.2007.00166.x.
43. Koutsoumanis KP, Kendall PA, Sofos JN. Effect of food processing-related stresses on acid tolerance of Listeria monocytogenes. Appl Enviorn Microb 2003;69:7514–6. https://doi.org/10.1128/AEM.69.12.7514-7516.2003.
44. Liu S, Ozturk S, Xu J, Kong F, Gray P, Zhu MJ, et al. Microbial validation of radio frequency pasteurization of wheat flour by inoculated pack studies. J Food Eng 2018;217:68–74. https://doi.org/10.1016/j.jfoodeng.2017.08.013.
45. Xu J, Liu S, Tang J, Ozturk S, Kong F, Shah DH. Application of freeze-dried *Enterococcus faecium* NRRL B-2354 in radio-frequency pasteurization of wheat flour. LWT-Food Sci Technol 2018;90:124–31. https://doi.org/10.1016/j.lwt.2017.12.014.

Supplementary material: The online version of this article offers supplementary material https://doi.org/10.1515/ijfe-2019-0388